Fuel-Economic Flight Optimization for Descent and Approach Phases

Yiming Zhao* and Panagiotis Tsiotras†

School of Aerospace Engineering, Georgia Institute of Technology, Atlanta GA 30332-0150

This paper presents a computationally efficient flight optimization method for improving the fuel economy of a fixed-wing aircraft following a landing path during the descent and approach phases. The problem is converted to an optimal control problem with one energy state variable, subject to state and control input constraints along the path. It is shown that the solution to the energy-optimal path following problem provides a good approximation to the minimum-fuel problem, hence, it can be used for improving the fuel economy. Compared to standard numerical optimization techniques, the proposed method is more suitable for onboard real-time trajectory optimization because of its guaranteed convergence, and computational efficiency. Numerical examples are presented to demonstrate the validity of the proposed approach, and its capability for improving fuel economy during the landing phase.

Nomenclature

s	Path coordinate, m
t	Time, s
s_f	Path length, m
t_f	Final time, s
x, y, z	Position, m
v	Speed, m/s
γ	Path angle, rad
ψ	Heading angle, rad
m	Mass, kg
g	Gravity acceleration, m/s^2
T	Thrust, N
ϕ	Bank angle, rad
C_L	Lift coefficient
C_D	Drag coefficient
C_{D_0}	Zero lift drag coefficient
K	Induced drag coefficient
S	Wing surface area, m^2
ρ	Air density, kg/m^3
$C_{L_{\min}}$	Minimum lift coefficient
$C_{L_{\max}}$	Maximum lift coefficient
$\phi_{\min}$	Minimum bank angle, rad
$\phi_{\max}$	Maximum bank angle, rad
$T_{\min}$	Minimum thrust, N
$T_{\max}$	Maximum thrust, N
E	Kinetic energy per unit mass, J/kg
$\overline{g}_w$	Upper bound of kinetic energy, J/kg
$\underline{g}_w$	Lower bound of kinetic energy, J/kg

*Adjunct member research stuff. Mitsubishi Electric Research Laboratories, Cambridge, MA. This work was performed when the first author was a Ph.D student at the Georgia Institute of Technology. Email: yzhao7@gatech.com

†Dean's Professor, AIAA Fellow, Email: tsiotras@gatech.edu.

λ_t	Costate variable associated with t
T^*	Optimal thrust, N
E^*	Optimal specific kinetic energy, J/kg
C_L^*	Optimal lift coefficient,
ϕ^*	Optimal bank angle, rad
$\tilde{E}$	Singular specific kinetic energy arc, J/kg
$\tilde{T}$	Singular thrust control, N
D	Specific drag force, N/kg
$\tilde{D}$	Specific drag force along singular arc, J/kg
E_U^*	Minimum-time specific kinetic energy, J/kg
E_L^*	Maximum-time specific kinetic energy, J/kg
M_a	Mach number

I. Introduction

With rising fuel cost and environmental concern, it is desirable to improve the fuel efficiency of current aircraft operations subject to aircraft performance and scheduling constraints. Such a problem can be naturally cast as an optimal motion planning problem, which is a common problem encountered in many industrial and transportation systems, including robotic arms,[1–4] ground vehicles,[5–8] and aircraft.[9,10] Although optimal motion planning problems can be solved directly using numerical optimization techniques,[11–17] the number of the required computations may grow to impractical levels, especially for real-time applications. Hence, a hybrid approach is commonly adopted in practice, according to which the motion planning task is decomposed into multiple levels.[18,19] At the higher level, only the geometric aspects of the path are considered, while the lower (path-tracking) level deals with the system dynamics and the state and control constraints, and generates the time-parameterization of the path provided by the higher (geometric) level planner. This paper focuses on the aircraft path-tracking problem at the lower level. Therefore, throughout the paper, it is assumed that the flight path to be followed by the aircraft is given.

The assumption that the path is given, and its calculation is not part of the optimization process, is not as unusual or atypical as one may initially think. Commercial airliners during the terminal landing phase, are required to follow strict Air Traffic Control (ATC) rules, which guide the airplanes so as to follow "virtual" three-dimensional corridors all the way to the landing strip. Furthermore, since our approach leads to very fast computation of feasible trajectories, one can use the approach over new, locally modified paths repeatedly till a satisfactory path is found. See [20] for a computationally efficient approach to modify the original path such that it meets certain constraints. Finally, if necessary, the computed trajectories by the proposed approach can be used as an initial guess for a higher fidelity optimal trajectory generation solver to further improve the optimality.[21] Although from now on it is assumed that the path is given, this does not mean that the *trajectory* to be followed is given. A trajectory requires a time-parameterized path and it is, indeed, the main goal of this paper to provide such a time parameterization so as to meet certain optimality specifications.

Once the speed along a given path is determined, the aircraft's motion can be fully determined using inverse dynamics. Therefore, the aircraft optimal path following problem can be reduced to a speed optimization problem. The minimum-time aircraft path-following problem has been studied in [22, 23]. It is shown that the time-optimal path following solutions maximize pointwise the speed along the path, and do not contain any singular arcs. The optimal solution to this time-optimal problem can help achieve faster aircraft landing in case of an emergency.

When tracking time is not of primary concern, it is often desirable to minimize the fuel consumption during the flight. Due to the complexity of fuel consumption models, it is typically difficult to find an analytical solution minimizing the fuel consumption. However, because fuel consumption is closely related to the engine's mechanical work counteracting the effects of air drag, the issue of fuel efficiency can be addressed (at least approximately) by solving the minimum-energy problem. The validity of such a simplifying approximation is verified by numerical results later in this paper. Unlike the minimum-time solution, minimum-energy solutions usually contain singular control arcs in addition to the bang-bang control arcs. In the case of fixed travel time, which is most important for scheduled ATC operations,[5–7] the singular arc(s) cannot be computed directly, and a numerical procedure must be used to compute the singular arc(s) such

that the desired travel time and boundary conditions are satisfied.

When using standard numerical methods to solve singular optimal control problems, an approximate solution is usually obtained at first using standard numerical optimal control techniques, and then a control switching structure is guessed based on the approximate solution and the analytic expression of the singular control. Finally, the guessed switching structure is applied to solve the singular control problem.[24] These numerical methods are time-consuming, and require extensive knowledge and experience of the user to obtain the actual optimal solution. On the other hand, an analytical optimal control approach (such as in [5–7, 25]), although less general than purely numerical methods, can provide more accurate information about the singular arcs and switching times in the optimal solution, and thus it is more reliable and efficient.

In this paper we apply the energy-optimal speed optimization method in [25] to the aircraft path following solution to improve the fuel economy. A scalar functional optimization problem is formulated and solved semi-analytically using optimal control theory. Compared to the somewhat similar minimum-work problem for train operations,[5–7] the aircraft minimum-energy solution exhibits more complicated switching structures. Some of the basic results used in this paper were introduced in [23] (see also [22, 25]). To avoid unnecessary repetition, the reader will often be referred to [23, 25] for some of the missing details.

The rest of this paper is organized as follows: the aircraft dynamics is introduced in Section II. In Section III, the aircraft minimum-energy fixed TOA path-following problem is formulated as an optimal control problem, and the optimal solution is presented. Section IV describes two algorithms for the energy-optimal aircraft flight path following operation. Finally, the validity of the proposed methodology is tested using numerical experiments, and the results are presented at the end of the paper.

II. Aircraft Dynamics

The dynamics of a fixed-wing aircraft considered in this paper is given by the following equations of motion:[26]

$$\dot{x} = v\cos\gamma\cos\psi, \tag{1}$$

$$\dot{y} = v\cos\gamma\sin\psi, \tag{2}$$

$$\dot{z} = v\sin\gamma, \tag{3}$$

$$\dot{v} = \frac{1}{m}\left[T - F_D(C_L, v, z) - mg\sin\gamma\right], \tag{4}$$

$$\dot{\gamma} = \frac{1}{mv}\left[F_L(C_L, v, z)\cos\phi - mg\cos\gamma\right], \tag{5}$$

$$\dot{\psi} = -\frac{F_L(C_L, v, z)\sin\phi}{mv\cos\gamma}, \tag{6}$$

where x and y denote the position of the aircraft in the horizontal plane, z is the altitude, v is the aircraft speed, γ is the flight path angle, ψ is the heading angle, and ϕ is the aircraft bank angle. The aerodynamic lift force $F_L(C_L, v, z)$ and the drag force $F_D(C_L, v, z)$ are given by:

$$F_L\left(C_L, v, z\right) = \frac{1}{2}\rho(z)v^2SC_L, \tag{7}$$

$$F_D\left(C_L, v, z\right) = \frac{1}{2}\rho(z)v^2SC_D = \frac{1}{2}\rho(z)v^2S(C_{D_0} + KC_L^2), \tag{8}$$

where $\rho(z)$ is the air density given as a function of z, C_{D_0} and K are parameters describing the aerodynamic properties of the aircraft, and S is the main wing surface area. The drag coefficients C_{D_0} and K depend continuously on the Mach number, and hence, are continuous functions of the airspeed and the path length s. The control inputs in this model are the lift coefficient C_L, the bank angle ϕ, and the thrust T. It is required that the aircraft speed satisfies the bounds $v(s) \in [v_{\min}(z), v_{\max}(z)]$, where $v_{\min}(z)$ and $v_{\max}(z)$ are altitude-dependent minimum and maximum speeds, respectively, and

$$C_L \in [C_{L_{\min}}, C_{L_{\max}}], \quad \phi \in [\phi_{\min}, \phi_{\max}], \quad T \in [T_{\min}, T_{\max}], \tag{9}$$

where $C_{L_{\min}}$, $C_{L_{\max}}$, $\phi_{\min}$, $\phi_{\max}$, $T_{\min}$ and $T_{\max}$ are (possibly, path-dependent) bounds on the associated control inputs. It is assumed that $C_{L_{\min}} \leq 0 \leq C_{L_{\max}}$, $-\pi/2 < \phi_{\min} < 0 < \phi_{\max} < \pi/2$, $0 \leq T_{\min} < T_{\max}$,

and $\gamma \in (-\pi/2, \pi/2)$. These conditions are generic for a civil fixed-wing aircraft in normal/maneuverable flight.

Let now $(x(s), y(s), z(s))$ denote a three-dimensional geometric path, parameterized by its natural path length coordinate $s \in [s_0, s_f] \subset \mathbb{R}_+$. The main objective of this paper is to find a time-parameterization of the path, or equivalently, a function $s(t)$ with $s(0) = s_0$ and $s(t_f) = s_f$, where $t \in [0, t_f]$, and t_f is the desired TOA, such that the corresponding time-parameterized trajectory $\big(x(s(t)), y(s(t)), z(s(t))\big)$ minimizes the total energy, or mechanical work, while flying along the path, and without violating any state or control constraints. Since the path coordinate s is related to the speed v as follows

$$s(t) = \int_{t_0}^{t} v(\tau)\, \mathrm{d}\tau,$$

the key step for solving this problem is the optimization of the speed profile $v(s)$ along the path. For convenience of notation, let $E \triangleq v^2/2$ denote the specific kinetic energy per unit mass of the aircraft. It has been shown in Ref. [22] that the lift coefficient, the bank angle, the load factor, and the speed constraints can be reduced to lower and upper bounds on the specific kinetic energy E as follows:

$$E(s) - \overline{g}_w(s) \leq 0, \tag{10}$$

$$\underline{g}_w(s) - E(s) \leq 0, \tag{11}$$

for all $s \in [s_0, s_f]$, where $\overline{g}_w(s)$ and $\underline{g}_w(s)$ are path-dependant bounds on the specific kinetic energy, which are determined from the path geometry, and the constraints on the speed, the bank angle and the lift coefficient. The derivative of E satisfies the following ordinary differential equation:[22]

$$E'(s) = \frac{T(s)}{m} - D(E(s), s) - g \sin\gamma, \tag{12}$$

where the prime denotes the derivative with respect to s, and

$$D(E, s) = c_1(E(s), s)E(s) + \frac{c_2(E(s), s)}{E(s)} + c_3(E(s), s), \tag{13}$$

with

$$c_1(E, s) \triangleq \frac{C_{D_0}(E, s)\rho(s)S}{m} + \frac{4K(E, s)m}{\rho(s)S}\left(\gamma'^2(s) + \cos^2\gamma(s)\psi'^2(s)\right), \tag{14}$$

$$c_2(E, s) \triangleq \frac{K(E, s)mg^2\cos^2\gamma(s)}{\rho(s)S}, \tag{15}$$

$$c_3(E, s) \triangleq \frac{4K(E, s)m\gamma'(s)g\cos\gamma(s)}{\rho(s)S}. \tag{16}$$

It is assumed that $D(E, s)$ is continuous with respect to s. It is also assumed that $\partial D/\partial E \neq 0$ and is differentiable with respect to s, except for at most a finite number of points in $[s_0, s_f]$. Once the optimal specific kinetic energy $E^*(s)$ is obtained, the optimal thrust profile $T^*(s)$ along the path can be determined using equation (12). Subsequently, the other optimal control inputs can also be computed using inverse dynamics as follows:

$$\phi^*(s) = -\arctan\left(\frac{\cos\gamma(s)\psi'(s)}{\gamma'(s) + g\cos\gamma(s)/v^{*2}(s)}\right), \tag{17}$$

$$C_L^*(s) = \frac{2m}{\rho(s)S\cos\phi^*(s)}\left(\gamma'(s) + \frac{g\cos\gamma(s)}{v^{*2}(s)}\right). \tag{18}$$

III. Problem Formulation and the Energy-Optimal Solution

In this section, the energy-optimal aircraft path-following problem with fixed TOA is formulated as a minimum-energy speed optimization problem, which has been studied in [25], and the optimal solution is presented.

Most modern civil airliners are powered by high-bypass turbofan engines for better fuel economy. The fuel consumption rate for this type of engine is given by[27]

$$\dot{f} = -\eta T, \tag{19}$$

where f is the fuel weight, η is the *installed thrust specific fuel consumption*, which varies with airspeed, altitude, type of engine, and throttle conditions, and it is given by

$$\eta = (a + bM_a)\sqrt{\eta_0/(1 + cM_a^2)}, \tag{20}$$

where M_a is the Mach number and a, b, c are constants depending on the engine type. In (20), $\eta_0 = \eta_0(z, M_a)$ varies with altitude and Mach number and can be determined from look-up data tables.[27] The fuel consumption models for other types of jet engines are similar to equations (19) and (20), but with different parameters.

With the above model, the fuel consumption during the landing phase can be estimated by

$$J_f = \int_{t_0}^{t_f} -\dot{f}(t)\,\mathrm{d}t = \int_{t_0}^{t_f} \eta(t)T(t)\,\mathrm{d}t. \tag{21}$$

From (21) it is clear that the minimum-fuel problem is equivalent to the minimization of the weighted thrust history, where the weight $\eta(t)$ is given in (20). The solution to this problem requires the use of purely numerical techniques. To avoid this difficulty, this paper seeks to minimize, instead, the total energy (mechanical work) required to fly along the path, which is given by

$$J_w = \int_{t_0}^{t_f} v(t)T(t)\,\mathrm{d}t = \int_{s_0}^{s_f} T(s)\,\mathrm{d}s. \tag{22}$$

As demonstrated in Ref. [28], the optimal speed profile of the minimum-fuel optimization problem contains singular arcs on which most of the fuel-saving is achieved. It was observed in our numerical studies that the air speed changes slowly along these singular arcs, in which case the singular arcs of the fuel-optimal problem can be approximated by those of the energy-optimal problem. As a result, the minimization of the energy cost function (22) is expected to provide a reasonably good approximation to the fuel optimization problem (21). This is verified by the numerical results in Section V. Therefore, once the path dependent specific kinetic energy bounds $\overline{g}_w$ and $\underline{g}_w$ are obtained using the method introduced in Ref. [23], the minimum-energy speed optimization method in Ref. [25] can be applied to improve flight fuel economy by minimizing (22).

It needs to be pointed out that the minimum-energy speed optimization method in Ref. [25] does not address the system's mass change in the path following process. Since the the change of mass due to fuel consumption is usually negligible when compared to the total mass of the aircraft during the descent and approach phases, we can assume that m is constant during the landing phase, and apply results in Ref. [25] directly. The validity of such an assumption is justified in Ref. [28], which reported that the mass change has little influence on the fuel-optimal trajectory during the climb and descent phases. However, this assumption would be invalid during a long cruise phase [29], therefore the fuel economy improvement method discussed in this paper is not applicable to the long cruise phase.

To account for the fixed final time, the flight time t is treated as a state variable in an augmented system with the additional differential equation

$$t'(s) = \frac{1}{\sqrt{2E(s)}}.$$

With the above assumptions, the minimum-energy aircraft path-following problem with fixed TOA can be formulated as an optimal control problem involving two differential equations, two algebraic constraints, four boundary conditions, and two control constraints, as follows:

Problem 1 (Minimum-energy path-following problem with fixed TOA).

$$\min_{T} \quad \int_{s_0}^{s_f} T(s)\,\mathrm{d}s, \tag{23}$$

$$\text{subject to} \quad E'(s) = \frac{T(s)}{m} - D(E(s), s) - g\sin\gamma(s), \tag{24}$$

$$t'(s) = \frac{1}{\sqrt{2E(s)}}, \tag{25}$$

$$E(s) - \overline{g}_w(s) \le 0, \tag{26}$$

$$\underline{g}_w(s) - E(s) \le 0, \tag{27}$$

$$E(s_0) = v_0^2/2, \tag{28}$$

$$E(s_f) = v_f^2/2, \tag{29}$$

$$T_{\min}(s) \le T(s) \le T_{\max}(s), \tag{30}$$

$$t(s_0) = 0, \tag{31}$$

$$t(s_f) = t_f. \tag{32}$$

Suppose that the optimal specific kinetic energy E^* contains a singular arc represented by $\tilde{E}$, i.e., $E^*(s) = \tilde{E}(s)$ on some subinterval of $[s_0, s_f]$. For notational convenience, let us denote

$$\frac{\partial^k \tilde{D}}{\partial E^k} = \left.\frac{\partial^k D}{\partial E^k}\right|_{(\tilde{E}(s),s)}, \qquad k = 1, 2,$$

and let λ_t^* be the optimal costate value, then it can be shown that along the singular specific kinetic energy profile, we have[25]

$$P(\tilde{E}(s), s) = \lambda_t^*, \tag{33}$$

where

$$P(E, s) = 2\sqrt{2}mE^{3/2}\left.\frac{\partial D}{\partial E}\right|_{(E,s)} \tag{34}$$

for any $E > 0$. By the differentiability and non-zero assumption on $\partial D/\partial E$ in Section II, E as defined by (33) is differentiable with respect to s except possibly a finite number of points.

The following assumption on the function D is essential for the main results in Ref. [25] to hold.

Assumption 1. For all $E \in [v_{\min}^2/2, v_{\max}^2/2]$ and $s \in [s_0, s_f]$:

$$\frac{\partial^2 D(E, s)}{\partial E^2} + \frac{3}{2E}\frac{\partial D(E, s)}{\partial E} > 0 \tag{35}$$

Once the singular kinetic energy profile $\tilde{E}$ is determined, the singular control $\tilde{T}$ along $\tilde{E}$ can be obtained by

$$\tilde{T}(s) = m\left(\tilde{E}'(s) + D(\tilde{E}(s), s) + g\sin\gamma(s)\right) \tag{36}$$

where $\tilde{E}(s)$ is differentiable with respect to s. If $\tilde{E}$ is not differentiable at s (which may happen only at a finite number of points), the value of $\tilde{T}(s)$ can be defined by a continuation from the proper direction (left or right). Suppose there exists $(s_a, s_b) \subseteq [s_0, s_f]$ such that $E^*(s) = \tilde{E}(s)$ but $\tilde{T}(s) > T_{\max}$ or $\tilde{T}(s) < T_{\min}$. It follows that the corresponding optimal thrust profile cannot contain any singular thrust subarc. Therefore, in the sequel it is assumed that $\tilde{T}(s) \in [T_{\min}, T_{\max}]$ for all $s \in (s_a, s_b)$. This assumption is valid as long as the aircraft is in a normal flight condition, and the path is smooth enough, in the sense that the path angle and the heading angle change slowly along the path.

The main result regarding the energy-optimal speed optimization in Ref. [25] is given by Theorem III.1 below. The proof of the theorem takes advantage of the optimal solution of a relaxed problem, which is formed by relaxing the state constraints on some carefully selected intervals. Then it is shown that this solution satisfies the state constraints in the original Problem 1, hence is also the optimal solution to Problem 1. The reader is referred to Ref. [30] for detailed proof.

Theorem III.1. Let E_U^* and E_L^* be the minimum-time and maximum-time specific kinetic energy solutions, respectively. Suppose there exists a real number λ_t and a function $\tilde{E}$ given by $P(\tilde{E}(s), s) = \lambda_t$ for all $s \in [s_0, s_f]$, such that the specific kinetic energy E^* given by

$$E^*(s) = \begin{cases} E_L^*(s), & s \in \Gamma_L, \\ \tilde{E}(s), & s \in [s_0, s_f] \setminus (\Gamma_U \cup \Gamma_L), \\ E_U^*(s), & s \in \Gamma_U \end{cases} \tag{37}$$

satisfies the desired TOA, where $\Gamma_U = \{s | E_U^*(s) < \tilde{E}(s),\ s \in [s_0, s_f]\}$, and $\Gamma_L = \{s | E_L^*(s) > \tilde{E}(s),\ s \in [s_0, s_f]\}$. Then E^* is the optimal solution to Problem 1.

It is interesting to note that although the switching structure of the optimal solution to Problem 1 can be quite complicated, the expression of the optimal specific kinetic energy E^* can be written in a very succinct form in (37), as a combination of the minimum-time solution, the maximum-time solution, and energy-saving singular arcs.

Remark 1. Before applying the energy-optimal speed profile optimization method in Ref. [25] to the optimal flight path following problem, it is necessary to first verify condition (35), because this condition is essential for the optimality of singular arc, which form the basis for analysis in [25].

Given the importance of condition (35), it is interesting to see how often this condition holds. To this end, note that since $E = v^2/2$, we have

$$\frac{\partial D}{\partial E} = \frac{1}{v}\frac{\partial D}{\partial v} \tag{38}$$

and

$$\frac{\partial^2 D}{\partial E^2} = \frac{1}{v}\frac{\partial}{\partial v}\left(\frac{\partial D}{\partial E}\right) \tag{39}$$

$$= \frac{1}{v}\frac{\partial}{\partial v}\left(\frac{1}{v}\frac{\partial D}{\partial v}\right) \tag{40}$$

$$= \frac{1}{v^2}\frac{\partial^2 D}{\partial v^2} - \frac{1}{v^3}\frac{\partial D}{\partial v} \tag{41}$$

Therefore condition (35) can be written equivalently as

$$\frac{1}{v^2}\frac{\partial^2 D}{\partial v^2} - \frac{1}{v^3}\frac{\partial D}{\partial v} + \frac{3}{v^2}\frac{1}{v}\frac{\partial D}{\partial v} = \frac{1}{v^2}\frac{\partial^2 D}{\partial v^2} + \frac{2}{v^3}\frac{\partial D}{\partial v} > 0.$$

It follows that condition (35) holds when

$$\frac{\partial^2 D}{\partial v^2} > 0 \quad \text{and} \quad \frac{\partial D}{\partial v} > 0,$$

which is typically the case for atmospheric flight wherein the drag-airspeed curve is monotonically increasing and convex. In particular, when the airspeed of the aircraft is low (typically, < 0.6 Mach), the aerodynamic parameters C_{D_0} and K are approximately constant. In such a case, it can be verified analytically that (35) holds. When the Mach number of the aircraft is close to 1, the Mach number dependence of C_{D_0} and K usually cannot be neglected, and (35) need to be evaluated numerically in general.

Remark 2. Although the wind effect is not accounted for in the current formulation of the energy-optimal landing problem, it can be shown that the head or tail wind can be taken into consideration as long as $\overline{g}_w$ and $\underline{g}_w$ can be computed, and that the condition (35) is satisfied. While $\overline{g}_w$ can be easily obtained analytically, $\underline{g}_w$ can only be computed numerically when the wind effect can not be neglected. However, conservative estimation of $\underline{g}_w$ can be easily established. After $\overline{g}_w$ and $\underline{g}_w$ are computed, the minimum-time and maximum-time solutions can be computed, and the energy-optimal solution can be constructed as in (37). A comprehensive study of the wind effect including the cross-wind is not considered in this paper.

IV. An Energy-Optimal Path-Tracking Algorithm

Theorem III.1 characterizes the switching structure of the optimal solution to the aircraft energy-optimal path-tracking problem. Although E_U^* can be computed using the algorithm proposed in Ref. [22], and E_L^* can be computed in a similar manner, the optimal costate value λ_t^* is unknown. As a result, one is not readily able to choose the correct value of $\tilde{E}(s)$ for each $s \in [s_0, s_f]$ in order to construct the optimal specific kinetic energy according to (37). In this section a numerical algorithm is presented for solving Problem 1 by identifying the optimal costate value λ_t^*. This allows the computation of the associated function $\tilde{E}(s)$ from (33) and, subsequently, the optimal solution $E^*(s)$ from (37). To identify the constant λ_t^* and the associated singular arcs for a specific TOA, it is necessary to search among a family of extremals associated with the prescribed geometric path for the correct value of λ_t^*.

The algorithm for identifying the minimum-energy path-tracking control is given as follows:

Main Algorithm. *For the given path, aircraft parameters and constraints, compute the optimal solution for aircraft minimum-energy path-tracking operation with fixed TOA.*

1. Compute the state bounds $\overline{g}_w(s)$, $\underline{g}_w(s)$, and the functions $c_1(s)$, $c_2(s)$, $c_3(s)$ in Problem 1 as in Ref. [23].

2. Compute and store the values of $P\left(E(s), s\right)$ from equation (33) on a selected, adequately fine, mesh $\mathcal{M}$ over the domain $[s_0, s_f] \times [E_{\min}, E_{\max}]$, where $[E_{\min}, E_{\max}]$ covers the possible range of the specific kinetic energy.

3. Compute the minimum-time solution $E_U^*(s)$ and the maximum-time solution $E_L^*(s)$ using the algorithm in Ref. [22]. Let the corresponding minimum and maximum TOA be $t_{\min}$ and $t_{\max}$, respectively. Proceed to the next step if $t_{\min} < t_f < t_{\max}$. Otherwise, quit the algorithm since the desired TOA is not possible and the given problem does not have a solution.

4. Apply a Newton-Raphson algorithm with adjusted bounds of the solution[31] to find the optimal costate value λ_t^* such that $\tau_f = t_f$, where τ_f is given by Algorithm 1 below with $\lambda = \lambda_t^*$. Then the corresponding specific kinetic energy $E^*(s)$ associated with the costate value λ_t^*, which is returned by Algorithm 1, is the optimal solution with TOA equal to t_f.

5. Compute the optimal thrust $T^*(s)$, bank angle $\phi^*(s)$, and lift coefficient $C_L^*(s)$ histories using equations (12), (17), and (18), respectively.

Remark 3. If the first derivative of the optimal specific kinetic energy E^* as given by the Main Algorithm does not exist at some point $s \in (s_0, s_f)$, then the value of the optimal thrust T^* is not well-defined at s from (12). These are exactly the points where the derivative of E^* is discontinuous. The optimal thrust profile T^* is therefore discontinuous at those points. The limiting left/right values at these points of discontinuity of the thrust can be computed by the corresponding left/right limits of $E^{*\prime}$, which exist since E^* is a piecewise smooth function.

Step 4 of the Main Algorithm requires the computation of the optimal speed solution and the TOA for a specific extremal with costate value λ. This can be achieved using the following algorithm.

Algorithm 1 *Compute the TOA τ_f and the corresponding optimal specific kinetic energy profile $E^*(s)$ for a given λ value.*

1. Solve $P(\tilde{E}_\lambda(s), s) = \lambda$ for the function $\tilde{E}_\lambda(s)$ by interpolating the pre-computed and stored data of $P\left(E(s), s\right)$ for the given path on the mesh $\mathcal{M}$.

2. Compute the optimal specific kinetic energy $E^*(s)$ for the given λ using formula (37) along with the computed maximum-time specific kinetic energy $E_L^*(s)$ and minimum-time specific kinetic energy $E_U^*(s)$.

3. Compute the TOA τ_f for $E^*(s)$ using

$$\tau_f = \int_{s_0}^{s_f} \frac{1}{\sqrt{2E^*(s)}} \mathrm{d}s.$$

4. Return τ_f and $E^*(s)$.

In Step 1 of the Main Algorithm, one needs to first compute the derivatives of the prescribed position $(x(s), y(s), z(s))$ along the path with respect to the path coordinate s and obtain $x'(s)$, $y'(s)$, $z'(s)$,$x''(s)$, $y''(s)$, and $z''(s)$, where the double prime denotes the second derivative with respect to s. This can be done analytically when analytic expressions of $x(s)$, $y(s)$ and $z(s)$ are available. Otherwise, numerical differentiation schemes such as finite difference can be applied. After these derivatives are obtained, $\overline{g}_w(s)$, $\underline{g}_w(s)$, and the functions $c_1(s)$, $c_2(s)$, $c_3(s)$ can be obtained following Ref. [23].

According to the structure of the optimal specific energy profile in (37), it can be easily proved that the travel time τ_f of the energy-optimal solution decreases monotonically with increasing λ_t, since $\tilde{E}(s)$ increases monotonically with respect to λ_t for all $s \in [s_0, s_f]$ according to the definition of $\tilde{E}$ as in (33). In the Newton-Raphson algorithm with adjusted bounds used in Step 4 of the Main Algorithm, a bisection step is taken whenever the Newton-Raphson algorithm would take the solution outside the prescribed bounds. Since a bisection method is guaranteed to converge given the monotonicity property of the problem, such a hybrid method is also guaranteed to converge, and the Newton-Raphson steps can speed up the convergence.

It is noted that for a given set of aircraft parameters and a fixed flight path, both the minimum-time and maximum time solutions as well as the $P(E(s), s)$ values on the selected grid can be pre-computed and stored. Accordingly, the corresponding energy-optimal control with a specific TOA requires only a Newton-Raphson update in Step 4 of the Main Algorithm, which is computationally efficient. Therefore, one may easily reschedule the TOA based on the demand of air traffic control using the proposed method while still maintaining a fuel efficient flight.

V. Numerical Examples

In order to verify its accuracy, optimality and computation speed, the proposed energy-optimal tracking algorithm is tested using a three-dimensional landing trajectory, as shown in Fig. 1. The initial position of the aircraft is $(-135, -92, 6)$ km and the final position is $(0, 0, 0)$ km. The initial speed is v_0=220 m/s, and the final speed is v_f=95 m/s. Both the initial and final path angles are $0°$. The initial heading angle is $0°$, and the final heading angle is $-20°$. The horizontal projection of the trajectory contains two turning maneuvers, as shown in Fig. 2.

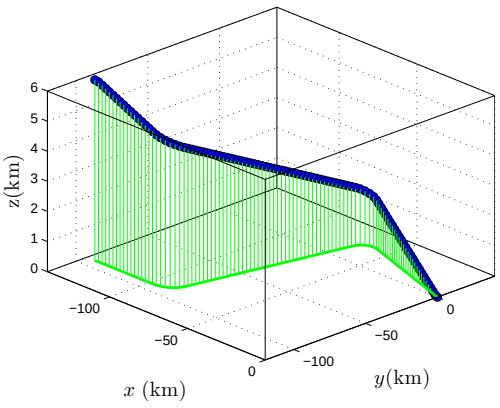

Figure 1. 3D Geometric Trajectory.

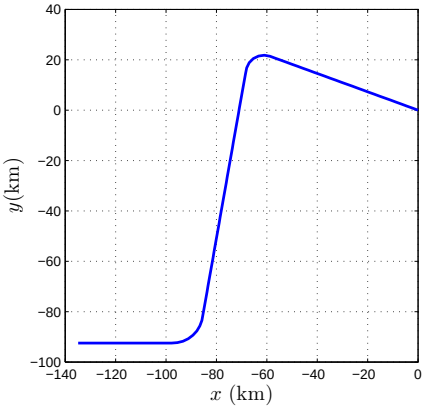

Figure 2. X-Y plane projection of the geometric trajectory.

The speed and control bounds considered during the time parameterization process are $M_a \leq 0.8$, where M_a is the Mach number, $C_{L_{\min}} = -0.47$, $C_{L_{\max}} = 1.73$, $\phi_{\min} = -15°$, $\phi_{\max} = 15°$, $T_{\min} = 0$. The wing surface area $S = 510.97\,\text{m}^2$, the mass $m = 288,938\,\text{kg}$. These data correspond approximately to a Boeing 747 aircraft. The aerodynamic parameters K and C_{D_0} are taken from Ref. [32] and stored in look-up tables. It has been verified numericaly that (35) hold for any subsonic flight along the path. The dependence of the maximum thrust $T_{\max}$ (N) on the altitude z and Mach number M_a is taken into account by the following

formula

$$T_{\max}(M_a, z) = (-0.007236z + 146.1968)(e^{-1.97967M_a+8.23} + 2133)\ \mathrm{N},$$

which fits approximately to the JT9D-7F engine maximum thrust data for a total of four engines.

The path is processed using the algorithm introduced in the previous section with different TOA requirements. Figures 3 and 4 show the optimal speed profiles for the minimum-energy aircraft path-tracking for several TOA values. It can be seen from these figures that with different TOA values t_f, different parts of the minimum-time and/or the maximum-time speed profile can be involved in the minimum-energy solution, together with the corresponding singular arcs. Figures 5 and 6 are the minimum-energy control histories for $t_f = 1300\,\mathrm{s}$ and $t_f = 1600\,\mathrm{s}$, respectively. In these figures, the throttle is the ratio of the actual thrust to the maximum thrust $T_{\max}$. It is clear that all solutions satisfy the speed and control constraints along the path.

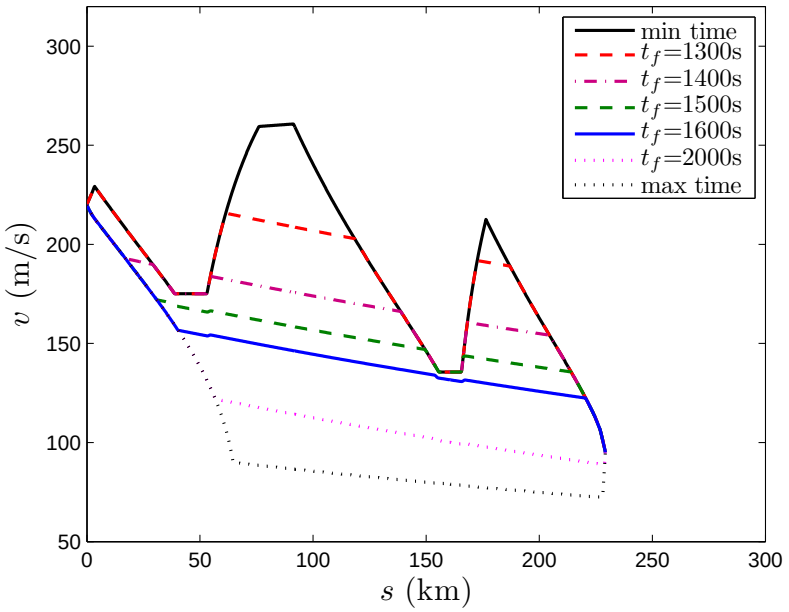

Figure 3. Energy-optimal speed profiles with different TOA, path coordinate domain.

To evaluate the fuel economy of the energy-optimal solution, a fuel-optimal control problem was solved using a numerical optimal control approach with the fuel consumption model (21) as the cost function. The constraints of the fuel-optimal control problem are identical to those of Problem 1. The fuel-optimal control problem was converted into a nonlinear programming problem via direct transcription,[11] and solved using the sparse nonlinear optimization software SNOPT.[33] The density function based mesh refinement method in Ref. [34] (DENMRA) was used to generate a mesh such that the state bounds (26) and (27) can be approximated more accurately with a limited number of grid points. The parameters for the computation of η_0 in equation (20) were stored in a look-up table, and were provided to the nonlinear optimization solver.

The same four cases shown in Fig. 3 ($t_f = 1300\,\mathrm{s}$, $1400\,\mathrm{s}$, $1500\,\mathrm{s}$, $1600\,\mathrm{s}$) were solved using the numerical optimal control approach for the minimum-fuel path-tracking problem, and the results were compared to those given by the energy-optimal path-tracking algorithm. The comparison of speed profiles are shown in Figs. 7 and 8. It is clear from these figures that the energy-optimal solutions are very close to the minimum-fuel solutions. Note that the singular arcs in the minimum-fuel problem cause numerical issues (oscillations along the singular arcs in Figs. 7 and 8). This is a well-known phenomenon when computing singular arcs using direct trajectory optimization methods.

To evaluate the effectiveness of the proposed energy-optimal operation method in terms of actual fuel-saving, the fuel consumptions of the energy-optimal results are simulated using the same fuel consumption model (21) as used by the numerical approach. The fuel consumption simulation results are compared with the fuel-optimal numerical optimization results in Talbe 1. As shown in the table, the simulated fuel consumption of the proposed method matches very well with the numerical optimization results, which

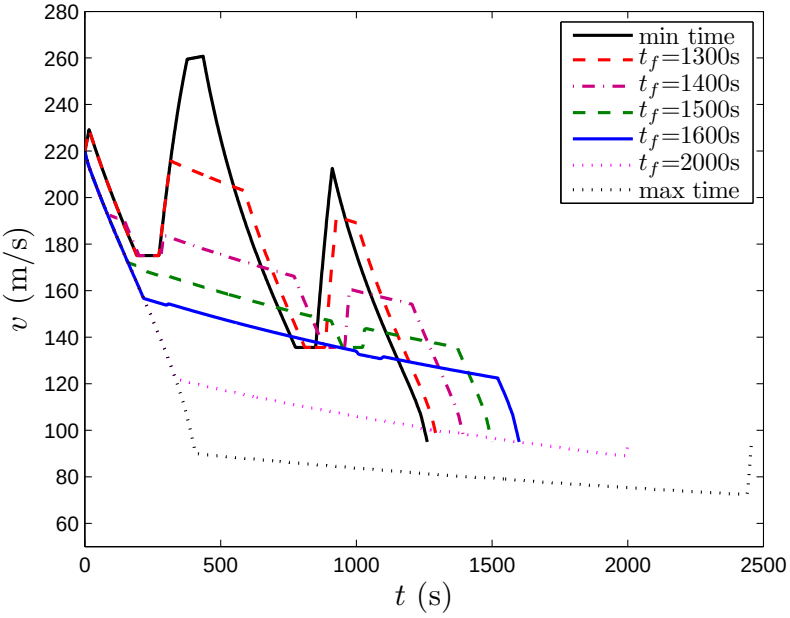

Figure 4. Energy-optimal speed profiles with different TOA, time domain.

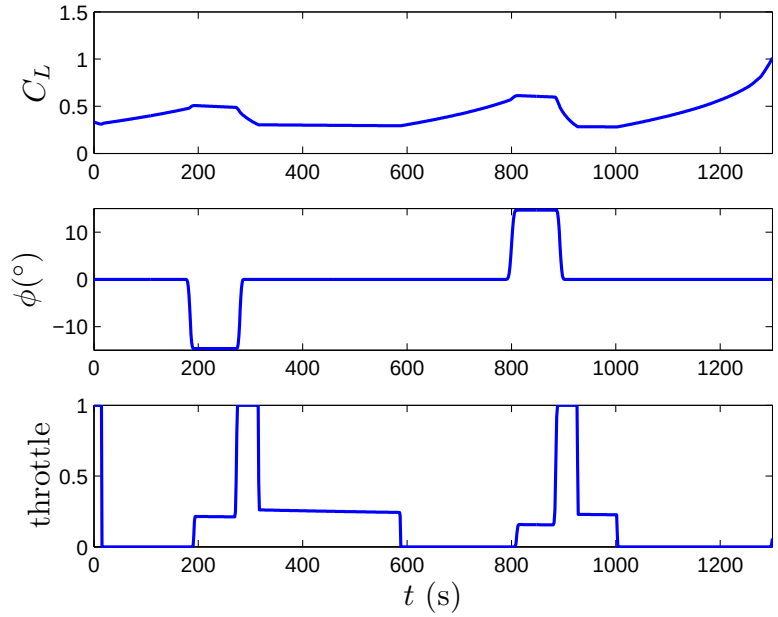

Figure 5. Energy-optimal control histories with $t_f = 1300$ s.

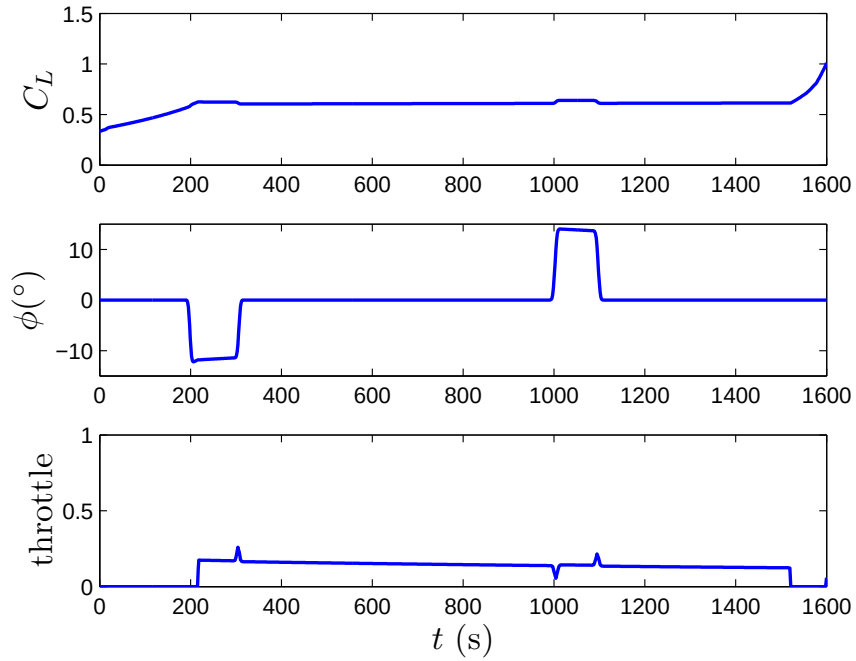

Figure 6. Energy-optimal control histories with $t_f = 1600$ s.

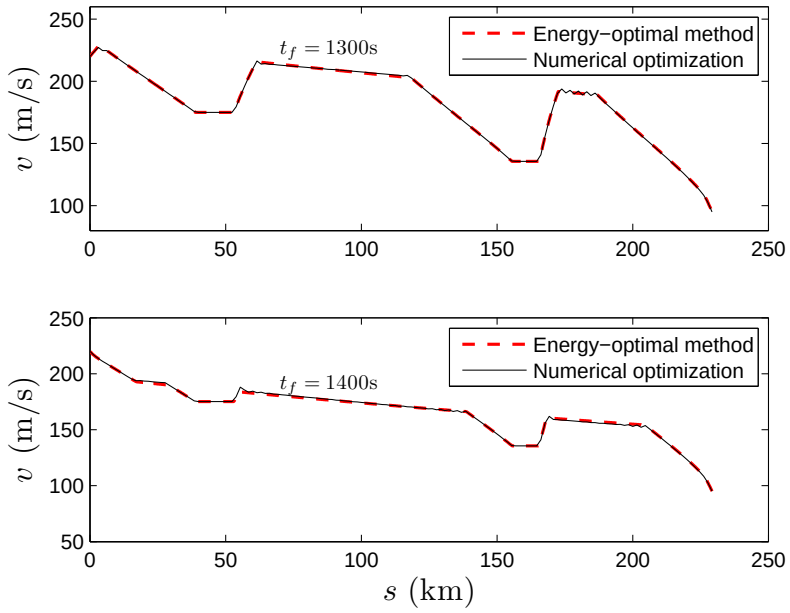

Figure 7. Comparison of fuel-optimal and energy-optimal speed profiles, $t_f = 1300$ s and $t_f = 1400$ s.

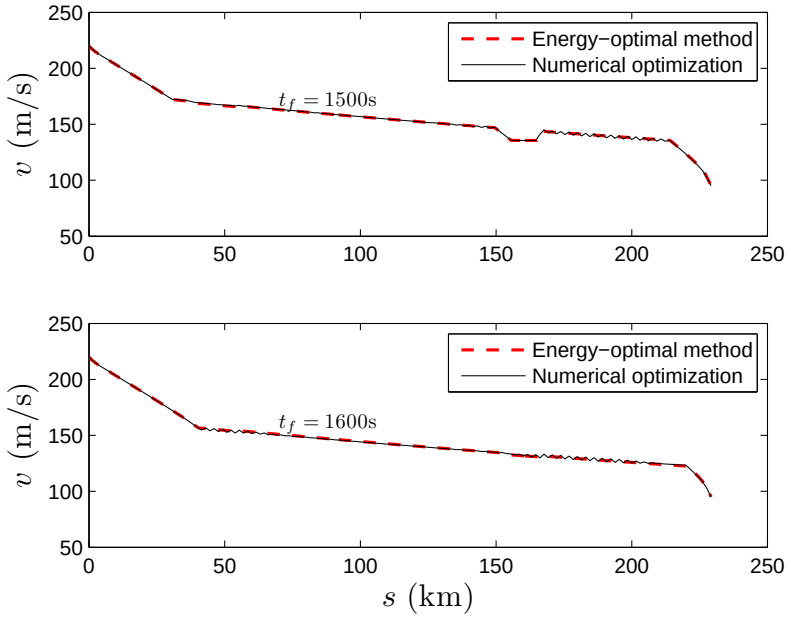

Figure 8. Comparison of fuel-optimal and energy-optimal speed profiles, $t_f = 1500$ s and $t_f = 1600$ s.

are obtained by minimizing the fuel consumption directly.

Table 1. Minimum fuel consumption comparison.

	Fuel consumption (kg)	
t_f (s)	NLP	Proposed method
1300	1809.2	1816.3
1400	1628.6	1632.9
1500	1612.0	1618.7
1600	1702.2	1704.8

Fig. 9 shows the relation between the optimal fuel consumption and total flight time when the aircraft is following the flight path in Fig. 1. The fuel consumptions in this figure are evaluated using the energy-optimal trajectories computed using the proposed method. It is clear that for the particular aircraft type and flight path considered, there is an optimal flight time which minimizes the fuel consumption. When the flight time is shorter than this optimal value, fuel savings can be achieved by delaying the flight time. Beyond this optimal point, however, the optimal fuel consumption increases significantly when extra delay is introduced.

The most appealing property of the proposed algorithm is its numerical efficiency. The computation times when using the standard numerical optimization approach is much longer than the one required by the proposed energy-optimal path-tracking algorithm: a Matlab implementation of the energy-optimal path-tracking control algorithm finds the optimal solution in 3-6 seconds, while the Nonlinear Programming solver takes at least 5 minutes (and for some cases, more than 20 minutes) to find a convergent fuel-optimal solution. The numerical efficiency of the algorithm allows the use of the proposed approach for computing good initial guesses for more accurate optimal trajectory generation solvers. In such a scenario, the semi-analytic solution provided by our approach can be further refined using more realistic, higher-fidelity aircraft models incorporating all effects neglected here, if needed. Previous results have shown a great increase in terms of numerical robustness and convergence of such trajectory generation solvers using this approach.[21,23]

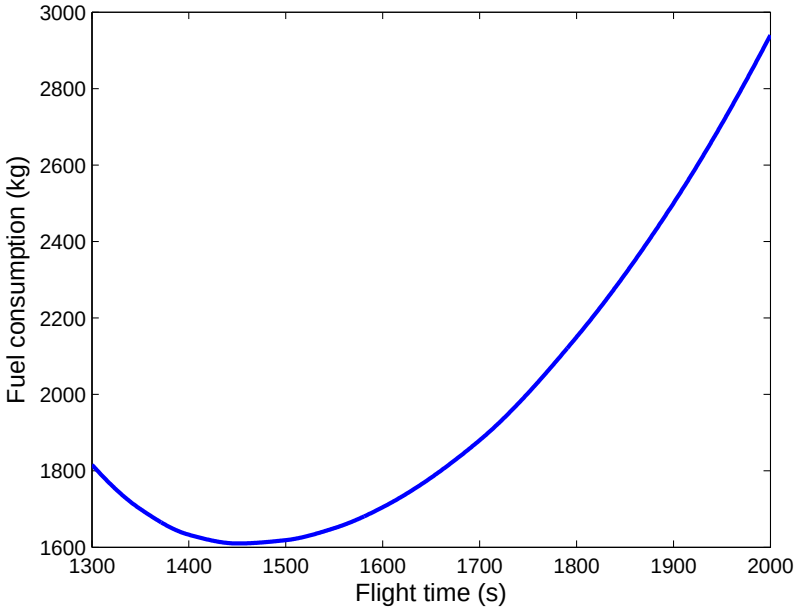

Figure 9. Minimum fuel consumption v.s. flight time.

VI. Conclusions

The paper applies the energy-optimal speed optimization method in Ref. [25] to improve the fuel economy of a fixed-wing aircraft following a given three-dimensional landing path with fixed time-of-arrival (TOA). As verified by the numerical optimization results, such a flight optimization approach is computationally efficient, hence is suitable for onboard real-time flight optimization. Furthermore, using the proposed method, the relation between the time-of-arrival and the corresponding minimum fuel consumption can be quantitatively determined for any given aircraft type and flight path, which can assist the planning of more fuel efficient flight schedules and landing paths. Although the discussions in this paper focus on the descent and approach phases of flight, the same approach will also apply to other short term operations, such as take-off and climb phases, when the change of the aircraft's mass is negligible.

References

[1]Shin, K. G. and McKay, N. D., "Minimum-Time Control of Robotic Manipulators with Geometric Path Constraints," *IEEE Transactions on Automatic Control*, Vol. AC-30, No. 6, June 1985, pp. 531–541.

[2]Pfeiffer, F. and Johanni, R., "A Concept for Manipulator Trajectory Planning," *IEEE Journal of Robotics and Automation*, Vol. RA-3, No. 2, April 1987, pp. 115–123.

[3]Shiller, Z. and Lu, H.-H., "Computation of path constrained time optimal motions with dynamic singularities," *Journal of Dynamic Systems, Measurement, and Control*, Vol. 114, No. 1, Mar 1992, pp. 34–40.

[4]Verscheure, D., Demeulenaere, B., Swevers, J., Schutter, J. D., and Diehl, M., "Time-Optimal Path Tracking for Robots: A Convex Optimization Approach," *IEEE Transaction on Automatic Control*, Vol. 54, No. 10, Oct. 2009, pp. 2318–2327.

[5]Asnis, I. A., Dmitruk, A. V., and Osmolovskii, N. P., "Solution of the Problem of the Energetically Optimal Control of the Motion of a Train by the Maximum Principle," *Computational Mathematics and Mathematical Physics*, Vol. 25, No. 6, 1985, pp. 37–44.

[6]Khmelnitsky, E., "On an Optimal Control Problem of Train Operation," *IEEE Transaction on Automatic Control*, Vol. 45, No. 7, Jul. 2000, pp. 1257–1265.

[7]Holett, P. G., Pudney, P. J., and Vu, X., "Local Energy Minimization in Optimal Train Control," *Automatica*, Vol. 45, No. 11, 2009, pp. 2692–2698.

[8]Velenis, E. and Tsiotras, P., "Minimum-Time Travel for a Vehicle with Acceleration Limits: Theoretical Analysis and Receding Horizon Implementation," *Journal of Optimization Theory and Applications*, Vol. 138, No. 2, 2008, pp. 275–296.

[9]Kelley, H. J., "Flight Path Optimization with Multiple Time Scales," *AIAA Journal of Aircraft*, Vol. 8, No. 4, 1971, pp. 238–240.

[10]Lu, P. and Pierson, B. L., "Optimal Aircraft Terrain-Following Analysis and Trajectory Generation," *Journal of Guidance, Control, and Dynamics*, Vol. 18, No. 3, 1995, pp. 555–560.

[11]Betts, J. T., *Practical Methods for Optimal Control using Nonlinear Programming*, PA: SIAM, 2001.

[12]Bulirsch, R., Montrone, F., and Pesch, H. J., "Abort Landing in the Presence of Windshear as a Minimax Optimal Control Problem, Part I: Necessary Conditions," *Journal of Optimization Theory and Applications*, Vol. 70, No. 1, 1991, pp. 1–23.

[13]Bulirsch, R., Montrone, F., and Pesch, H. J., "Abort Landing in the Presence of Windshear as a Minimax Optimal Control Problem, Part II: Multiple Shooting and Homotopy," *Journal of Optimization Theory and Applications*, Vol. 70, No. 2, 1991, pp. 223–254.

[14]Steinbach, M. C., Bock, H. G., and Longman, R. W., "Time-Optimal Extension and Retraction of Robots: Numerical Analysis of the Switching Structure," *Journal of Optimization Theory and Applications*, Vol. 84, No. 3, Mar. 1995, pp. 589–616.

[15]Cao, B., Dodds, G. I., and Irwin, G. W., "Constrained Time-Efficient and Smooth Cubic Spline Trajectory Generation for Industrial Robots," *IEE Proceedings Control Theory and Applications*, Vol. 144, No. 5, 1997, pp. 467–475.

[16]Choset, H., Lynch, K., Hutchinson, S., Kantor, G., Burgard, W., Kavraki, L., and Thrun, S., *Principles of Robot Motion-Theory, Algorithms, and Implementation*, The MIT Press, Cambridge, MA, Jun. 2005.

[17]Karelahti, J., Virtanen, K., and Öström, J., "Automated Generation of Realistic Near-Optimal Aircraft Trajectories," *Journal of Guidance, Control, and Dynamics*, Vol. 31, No. 3, 2008, pp. 674–688.

[18]Frazzoli, E., *Robust Hybrid Control for Autonomous Vehicle Motion Planning*, Ph.D. thesis, Massachusetts Institute of Technology, 2001.

[19]Plaku, E., Kavraki, L. E., and Vardi, M. Y., "Motion Planning With Dynamics by a Synergistic Combination of Layers of Planning," *IEEE Transactions on Robotics*, Vol. 26, No. 3, 2010, pp. 469–482.

[20]Zhao, Y. and Tsiotras, P., "A Quadratic Programming Approach to Path Smoothing," *American Control Conference*, San Francisco, CA, June 29-July 1 2011.

[21]Bakolas, E., Zhao, Y., and Tsiotras, P., "Initial Guess Generation for Aircraft Landing Trajectory Optimization," *AIAA Guidance, Navigation, and Control Conference*, No. AIAA Paper 2011-6689, Portland, OR, August 8-11 2011.

[22]Zhao, Y. and Tsiotras, P., "Time-Optimal Parameterization of Geometric Path for Fixed-Wing Aircraft," *Infotech@Aerospace Conference*, AIAA-2010-3352, Atlanta, GA, 2010.

[23]Zhao, Y. and Tsiotras, P., "Time-Optimal Path Following for Fixed-Wing Aircraft," *Journal of Guidance, Control, and Dynamics*, Vol. 36, No. 1, Janurary 2013, pp. 83–95.

[24]Vossen, G., Rehbock, V., and Siburian, A., "Numerical solution methods for singular control with multiple state dependent forms," *Optimization Methods and Software*, Vol. 22, No. 4, 2007, pp. 551–559.

[25]Zhao, Y. and Tsiotras, P., "Speed Profile Optimization for Optimal Path Following," *American Control Conference*, June 17-19 2013.

[26]Miele, A., *Flight Mechanics, Vol. I: Theory of Flight Paths*, Addison-Wesley, Reading, MA, 1962.

[27]Mattingly, J. D., Heiser, W. H., and Pratt, D. T., *Aircraft Engine Design*, AIAA, 1987.

[28]Burrows, J. W., "Fuel-optimal aircraft trajectories with fixed arrival times," *Journal of Guidance, Control, and Dynamics*, Vol. 6, No. 1, Jan.-Feb. 1983, pp. 14–19.

[29]Franco, A., Rivas, D., and Valenzuela, A., "Minimum-Fuel Cruise at Constant Altitude with Fixed Arrival Time," *Journal of Guidance, Control, and Dynamics*, Vol. 33, No. 1, Jan.-Feb. 2010, pp. 280–285.

[30]Zhao, Y., *Efficient and Robust Aircraft Landing Trajectory Optimization*, Ph.D. thesis, School of Aerospace Engineer, Georgia Institute of Technology, 2012.

[31]Press, W. H., Teukolsky, S. A., Vetterling, W. T., and Flannery, B. P., *Numerical Recipes: The Art of Scientific Computing*, Cambridge University Press, 3rd ed., Aug. 2007.

[32]Mair, W. A. and Birdsall, D. L., *Aircraft Performance*, Cambridge Aerospace Series, Cambridge University Press, 1996, pp. 255.

[33]Gill, P. E., Murray, W., and Saunders, M. A., "SNOPT: An SQP Algorithm for Large-scale Constrained Optimization," Numerical analysis report 97-2, University of California, San Diego, La Jolla, CA, 1997.

[34]Zhao, Y. and Tsiotras, P., "Density Functions for Mesh Refinement in Numerical Optimal Control," *Journal of Guidance, Control, and Dynamics*, Vol. 34, No. 1, Jan.-Feb. 2011, pp. 271–277.